



Treball final de grau

**GRAU DE
MATEMÀTIQUES**

**Facultat de Matemàtiques
Universitat de Barcelona**

Ordre i Caos en Ecologia

Arnau Via Martínez-Seara

Director: Alejandro Haro Provinciale
Realitzat a: Departament de Matemàtica
Aplicada i Anàlisi. UB

Barcelona, 15 de Juny de 2012

Order and Chaos in Ecology

Arnau Via M-Seara

June 20, 2012

Contents

Introduction	2
1 The biological problem	5
1.1 The three-species food chain model	5
1.2 The SEIR model	6
2 Some basic Concepts of Dynamical Systems	8
2.1 Dynamical Systems	8
2.2 Invariant objects	8
2.3 The Poincare Map	9
2.4 ω and α limit sets	9
2.4.1 Attractors	10
2.5 Bifurcations	10
2.5.1 Hyperbolic points and Hartman-Grobman Theorem	11
2.5.2 Non-hyperbolic points. Bifurcations	12
2.6 Transition to chaos	15
3 Chaos and Symbolic Dynamics	16
3.1 Symbolic dynamics	18
3.2 Topological conjugacy	19
3.3 Strange attractor	20
3.3.1 Lyapunov Exponents	21
3.3.2 Fractal Dimension	21
4 Numerical Methods	22
4.1 Numerical Integrators of odes	22
4.1.1 Runge-kutta	22
4.1.2 The Taylor method	22
4.2 Other standard numerical tools	24
4.2.1 Zero finders	24
4.2.2 Numerical Differentiation	26

5	Analysis of the Models	27
5.1	Local behaviour	27
5.2	Transition to chaos	30
5.3	Strange Attractor	34
6	Chaos in real ecological systems	41

Introduction

The motivation of this work comes from the reading of the chapters:

- Com entendre el comportament no predictable dels sistemes deterministes (C. Simó).
- Caos espaciotemporal en ecosistemes (R.V. Solé).
- Buscant l'ordre ocult dels sistemes biològics (J. Bascompte).

of the book "Order and Chaos in ecology"[1], devoted to explain how the knowledge of the phenomenon known as "deterministic chaos" has made a qualitative change in the way scientists of this area look at the problems in ecology.

From the point of view of biologists, that are interested in studying biological phenomena and be able to make predictions, the use of mathematical models has been a source of progress. Once one has a mathematical complex model which tries to describe the evolution of certain species, of an epidemic, the beats a beetle or the waves of human brain, dynamical systems help to simplify the study of such phenomena, mainly because its tools are designed to make predictions about the past and the future of the system.

It is known that, after simulating these mathematical models, and using the Dynamical Systems techniques which allow to reconstruct the attractors of the system just using real data, one has found in lots of these models the existence of deterministic Chaos. Therefore, a natural question has arised in the scientific (biological, ecological) community: Once a mathematical model shows to present deterministic Chaos, is this Chaos really present in nature, that is, does Chaos really exist in the real phenomenon modeled? Or it is just a consequence of the errors due to the modelization of the phenomenon, and the errors coming from the me measurements of the parameters and the numerical approximations needed to work with the system?

This is the starting point of the chapters of the book we have focused in. Answering the question is a difficult task. Nevertheless, we will briefly explain in this work how modern techniques, like the reconstruction of the attractors of a system from real data using *delay plots*, show clearly, an evidence: it is not true the quite extended in the past idea that nature tends to simple equilibrium states, like fixed points or periodic orbits. This discovery made a revolutionary change in the way scientists looked at nature realising that often they have to deal with unpredictibility.

This fact makes even more interesting the mathematical approach to deterministic Chaos, a fascinating area in itself, and it is with this perspective that we will make a systematic study of attractors from a mathematical point of view. Attractors are the most important sets from an a ecological point of view: there are sets were the dynamics of the system ends in a natural way and therefore, they are the sets were, with highest probability, the orbits of our system and therefore the real phenomena, will stay.

As we will restrict ourselves to a mathematical study, we will assume from now on that the models we are using are correct models, and our main goal will be to find and study their attractor sets. To do it, we will use mainly numerical tools, that is, we will try to reproduce these sets using accurate numerical simulations, and we will study their

properties. We will use techniques like the Poincaré map and graph analysis which will help us to simplify a little the study of these sets, that can be, in general, quite complex.

We will mainly work in a classical model: the trophic chain model of three species, but we will also give some issues about another model: the classical epidemic model SEIR. Both models depend on several parameters. We will fix several parameters into realistic values and vary one of them that will be very significant in the model. In fact, we will see that, varying slightly this parameter, the system undergoes very different dynamical behaviours. It will undergo several bifurcations (infinitely many!) and even chaotic behavior in some cases. Besides the reconstruction of the attractor of the system, we will also reconstruct a bifurcation cascade, a fascinating phenomenon which occurs in systems showing chaotic behaviour. Notably, this chaotic behaviour was first observed in (apparently) very simple models such as the logistic family. We will give a brief description of the dynamics of this family in section 3.

The work is organized in the following way. First, in Section 1, we will present the two ecological models. Later, in Section 2, we will introduce, in an informal way, some concepts and Theorems of Dynamical Systems, as well of some numerical methods (some of them very recent and quite sophisticated), necessary to follow the numerical approach done in the work.

Section 3 is devoted to present the tools used to understand deterministic chaos. This section contains the basic definitions like chaotic system, symbolic dynamics, and strange attractors. All the concepts and results are given and applied to classical one-dimensional dynamical system: the logistic map.

In Section 5 we analyse the obtained results and make some conclusions. Is in this chapter were we will make the mathematical-numerical machinery to work in order to understand all the phenomena of the system. All the results presented in this section have been obtained by myself. To this end I have written all the codes necessary to obtain the numerical simulations presented and the graphics: Taylor method to numerically integrate the 3-dimensional Ordinary Differential Equations of the models, Newthon method and numerical differentiation to built the Poincaré map and its derivative and its fixed points, a numerical approximation of the first period-doubling bifurcations, and delay plots to show the dynamics of the systems. It is also in this section were we will find the strange attractors, we reproduce the results of the book and compute new ones.

We devote the last section to present the arguments the authors use to justify that the observed Chaos is also present in the real phenomenon in nature.

1 The biological problem

In this section we will explain the problems we are going to study. They are two classic ecological problems: the **Three-species Food chain model**, which models a trophic chain, and the **SEIR model**, a model about the progress of an epidemic. We have obtained both models from [1]

1.1 The three-species food chain model

The first model deals with the "trophic chain of three species". We consider three species X, Y, Z , where Z is a predator for Y and that Y is a predator for a prey X . This model is used to model the evolution of three different species connected by a food chain, or also to models three groups of species with the same preys and predators. The flow of the model is:

$$\begin{aligned}\dot{X} &= R_0X\left(1 - \frac{X}{K_0}\right) - C_1F_1(X)Y \\ \dot{Y} &= F_1(X)Y - F_2(Y)Z - D_1Y \\ \dot{Z} &= C_2F_2(Y)Z - D_2Z\end{aligned}$$

where $\dot{} = \frac{d}{dt}$ and $F_i(U) = \frac{A_iU}{B_i+U}$ representing the functional response.

The constant R_0 is the "intrinsic growth rate", K_0 is the "carrying capacity" of species X . The constants C_1^{-1}, C_2 are conversion rates of prey to predator for species Y and Z respectively, and D_1 and D_2 are constant death rates. A_i and B_i parametrize the functional response; B_i is the prey population level where the predation rate per unit prey is half its maximum value.

Let us observe that if $C_1 = 0$ the X variable follows, independently of the other variables, the logistic model.

We normalize the system using the non-dimensional variables:

$$\begin{aligned}x &= X/K_0 \\ y &= C_1Y/K_0 \\ z &= C_1Z/(C_2K_0) \\ t &= R_0T\end{aligned}$$

Denoting by $'$ the derivative respect to the new time t we obtain the system:

$$\begin{aligned}x' &= x(1 - x) - f_1(x)y \\ y' &= f_1(x)y - f_2(y)z - d_1y \\ z' &= f_2(y)z - d_2z\end{aligned}\tag{1}$$

with:

$$f_i(u) = \frac{a_iu}{1 + b_iu}$$

One can find the relations between the old and the new parameters in [3]. The values of the parameters are taken from real experiments and are given by:

$$a_1 = 5, a_2 = 0.1, b_2 = 2, d_1 = 0.4, d_2 = 0.01 \quad (2)$$

The parameter b_1 will have an important role in this study. We will see that varying b_1 the system will encounter several bifurcations and also chaotic behaviour. For this model the parameter b_1 varies in:

$$b_1 \in [2, 6.2]. \quad (3)$$

In this work we will make a numerical study of the dynamical system defined by system (1). We are interested in the attractors of the system when one varies the parameter b_1 . We will see that, for certain values of this parameter, the model (1) has strange attractors, that are objects with complex (fractal) geometry (see the formal definition of strange attractor in section 2.4.1). We will justify that this chaotic behaviour is not exists not only in the mathematical model we consider. Moreover we will see that this attractor and the chaotic behaviour generated in it corresponds to the real behavior of the species obtained by experiments.

1.2 The SEIR model

In this section we will present the SEIR model, which studies the progress of an epidemic in a large population, comprising many different individuals in various fields. The population diversity must be reduced to a few key characteristics which are relevant to the infection under consideration. For example, for many important infections there is a significant period of time during which the individual has been infected but is not yet infectious himself. During this latent period the individual is in compartment E (for exposed). It makes sense to divide the population into those who are susceptible (S) to the disease, those who are exposed (E), infected (I) and those who have recovered (R).

The model the authors consider is taken form [8]:

$$\left. \begin{aligned} \dot{S} &= \mu - \beta(t)SI - \mu S \\ \dot{E} &= \beta(t)SI - (\mu + \alpha)E \\ \dot{I} &= \alpha E - (\mu + \gamma)I \\ \dot{R} &= \mu R - \gamma I \end{aligned} \right\} \quad (4)$$

with the restriction $S + E + I + R = 1$, and then $S + E + I + R$ is a first integral of the system, which comes from the fact that S, E, I, R are proportions of the total population, which is normalized to be 1, and it neglects the birth-death processes.

$$\mu = 0.02, \alpha = 35.842, \gamma = 100$$

and others varying β_0 and β_1 .

$\beta(t) = \beta_0(1 + \beta_1 \cos(2\pi t))$ is the contact rate of the infection, and is modeled by a periodic function to emphasize that is seasonally varying in time (with period 1 year).

We will make also a numerical study of the dynamical system defined by (4). We will find the attractors of the system for certain values of the parameters.

2 Some basic Concepts of Dynamical Systems

The main goal of the work was perform a accurate numerical method to obtain the asymptotic behaviour of the orbits of the models considered. Nevertheless, as these systems present chaotic behaviour, it is very difficult to understand the numerical results without a deep knowledge of some concepts of dynamical systems.

Here we aim to give a list of these concepts adapted to our problem in an heuristic way:

2.1 Dynamical Systems

A **smooth continuous Dynamical System** is the tuple $(M, \phi(t, x), \mathbb{R})$ where M is a manifold, and $\phi(t, x)$ is a flow defined by an autonomous vector field X :

$$\frac{d}{dt}\phi(t, x) = X(\phi(t, x)), \quad \phi(0, x) = x.$$

The **orbit** of a point x is given by $\{\phi(t, x), t \in \mathbb{R}\}$ and we assume that the solutions are defined for any time. This is true, for instance, if M is compact.

A **discrete smooth Dynamical System** is the tuple (M, f, \mathbb{Z}) where M is a manifold, and $f : M \rightarrow M$ is a diffeomorphism. In this case the **orbit** of a point x is given by $\{f^n(x), n \in \mathbb{Z}\}$ or by $\{f^n(x), n \in \mathbb{N}\}$ in case f is not invertible.

2.2 Invariant objects

One of the first steps in the study of a Dynamical System is to find the **invariant objects**.

The simplest invariant objects in a continuous Dynamical System are **fixed points**:

- A point x is a **fixed point** of the vector field X if $\phi(t, x) = x$ and therefore $X(x) = 0$.
- A point x is a **fixed point** of the map f if $f(x) = x$.

Other simple invariant object in Dynamical Systems are **periodic orbits**

- The orbit of a point x is a **periodic orbit** if there exists $T \in \mathbb{R}$ such that $\phi(T, x) = x$. T is called the period of the orbit.
- A point x is a **periodic point** of the map f if there exists an $N \in \mathbb{Z}$ such that $f^N(x) = x$.

There is general definition for an invariant set of a Dynamical System.

- The set S is said to be invariant for the flow ϕ (f for the map), if $x \in S$ implies $\phi(t, x) \in S, \forall t \in \mathbb{R}$ ($f^n(x) \in S, \forall n \in \mathbb{Z}$).

2.3 The Poincaré Map

When a continuous dynamical system has a periodic orbit γ there is a natural way to associate a discrete Dynamical System to study the behaviour around γ : **The Poincaré Map**. This map was defined and studied in the subject of Ordinary Differential Equations.

Let γ be a periodic orbit of a Dynamical System (M, ϕ) , and Σ a transversal section to γ , then the Poincaré Map is defined as:

$$\begin{aligned} P : \Sigma &\rightarrow \Sigma \\ y &\rightarrow P(y) = \phi(\tau(y), y) \end{aligned}$$

where $\tau(y)$ is the minimum time t such that the flow $\phi(t, y) \in \Sigma$. Clearly $x^* = \gamma \cap \Sigma$ is a fixed point of P .

The Poincaré map has the advantage of reducing the dimension of the system. This makes it very convenient in numerical simulations.

2.4 ω and α limit sets

Another interesting sets for the study of Dynamical Systems are the ω and α -limit sets. These sets capture the long term behaviour of an orbit.

Given a continuous Dynamical System (M, ϕ) , a point x and an orbit $\gamma = \{\phi(t, x) \mid t \in \mathbb{R}\}$ through x , we call a point y an ω -limit point of γ if there exists a sequence t_n in \mathbb{R} so that

$$\begin{aligned} t_n &\nearrow +\infty \\ \lim_{n \rightarrow \infty} \phi(t_n, x) &= y \end{aligned}$$

Analogously we call y an **α -limit point** if there exists a sequence t_n in \mathbb{R} so that

$$t_n \searrow -\infty$$

$$\lim_{n \rightarrow \infty} \phi(t_n, x) = y$$

The set of all ω -limit points (α -limit points) for a given orbit γ is called ω -limit set (α -limit set) for γ and denoted $\lim_{\omega} \gamma$ ($\lim_{\alpha} \gamma$). Alternatively the limit sets can be defined as:

$$\lim_{\omega} \gamma := \bigcap_{s \geq 0} \overline{\{\phi(t, x) : t \geq s\}}$$

and

$$\lim_{\alpha} \gamma := \bigcap_{s \leq 0} \overline{\{\phi(t, x) : t \leq s\}}$$

The ω and α limit sets are invariant sets.

2.4.1 Attractors

Among the ω -limit sets, the most interesting ones are the **attractors**. On one hand they are the only ones you see on simulations. On the other hand the attractors are sets where the solutions of our systems end asymptotically, and as our systems model real phenomena, one of the most important goals is to be able to predict future states of the system, and they are very good candidates to describe the future behaviour of the system.

- A set S is an **attractor** if there exist a neighbourhood U of S such that S is the ω -limit set of all points of U .

Examples of attractors are attracting fixed points and periodic orbits, but there exist other attractor sets of higher dimension, and also of more complicated structure: the **Strange Attractors**.

The heuristic idea of strange attractor is an attractor set which has a complicated geometrical structure. We will explain in more detailed what is an strange attractor in section 3.3.

2.5 Bifurcations

One of the main purposes of this work to study the attractor sets, in particular fixed points, periodic points, and also strange attractors. To be able to study these strange sets we first introduce the concept of **bifurcation**. Roughly speaking a bifurcation occurs when small variations of the parameters give rise to a change in the qualitative dynamics

of the system. Very often a phenomenon called **cascade of bifurcations** leads the system from regular dynamics to what is called chaotic dynamics that we will explain in section 3.

But to introduce the concept of bifurcation we first need to talk about **hyperbolic points**.

2.5.1 Hyperbolic points and Hartman-Grobman Theorem

- If X is a vector field, x is a critical point, and $J = DX(x)$ is the Jacobian matrix, then the point x is said to be an **hyperbolic critical point** if for any $\lambda \in \text{Spec}(J)$ one has that $\Re(\lambda) \neq 0$.
- If f is a map, x is a fixed point and $J = Df(x)$, then the point x is said to be an **hyperbolic fixed point** if for any $\lambda \in \text{Spec}(J)$ one has that $\|(\lambda)\| \neq 1$.
- A periodic orbit of a continuous vector field is called hyperbolic if the corresponding Poincaré map has a hyperbolic fixed point.

The next theorem is about the local behaviour of a Dynamical System in the neighbourhood of a hyperbolic equilibrium point.

Theorem (Hartman-Grobman). *Let x be a hyperbolic fixed point of a vector field X or of a map f . Then there exists a neighbourhood U of x and neighbourhood V of 0, and an homeomorphism $h : V \rightarrow U$ such that:*

- $h(0) = x$
- h conjugates the flow ϕ of $\dot{x} = X(x)$ in U with the flow of $\dot{y} = DX(x)y$, that is:

$$h(e^{tDX(x)}y) = \phi(t, h(y))$$

- h conjugates the map f in U with the map $J(y) = Df(x)y$, that is:

$$h(J(y)) = f(h(y))$$

2.5.2 Non-hyperbolic points. Bifurcations

As Hartman-Grobman Theorem give us the behaviour near a hyperbolic critical point of a flow, or near a hyperbolic fixed point of a map and also near a hyperbolic periodic orbit, next step is to understand the behaviour near a point which is not hyperbolic.

Consider an autonomous system of ordinary differential equations

$$x' = f(x, \mu), \quad x \in \mathbb{R}^n, \quad \mu \in \mathbb{R}^p \quad (5)$$

where f is smooth.

A bifurcation occurs at parameter $\mu = \mu_0$ if there are parameter values μ_1 arbitrarily close to μ_0 with dynamics topologically inequivalent from those at μ_0 .

For example, the number or stability of equilibria or periodic orbits of f may change with perturbations of μ from μ_0 . One goal of bifurcation theory is to produce parameter space maps or bifurcation diagrams that divide the μ parameter space into regions of topologically equivalent systems. Bifurcations occur at points that do not lie in the interior of one of these regions.

The study of bifurcation theory is very difficult because to establish if two vector fields are topologically equivalent in whole phase space it is very complicated. That's why we will focus on local bifurcations, which refers to properties of a vector field near a point.

If system (5) has an hyperbolic critical point x_0 for $\mu = \mu_0$, by the *implicit function theorem*, the system will have a critical point $x(\mu)$, for μ close enough of μ_0 . Moreover $Df(x_0, \mu_0)$ and $Df(x(\mu), \mu)$ will have the same number of eigenvalues of positive and negative real part. Therefore both vector fields are topologically equivalent. We can conclude that if at $\mu = \mu_0$ system (5) has a hyperbolic critical point, μ_0 can not be a bifurcation value. Bifurcations then occur when one or several eigenvalues of the linearised system, have real part equal to 0. Analogue theory exist for maps around fixed points, but the condition would be that some of the eigenvalues have to be of modulus one.

The simplest bifurcation of critical point is when only one eigenvalue is equal to 0. This bifurcations can occur in one-dimensional vector fields depending on one parameter. That is, $n = p = 1$ in (5). The generic cases depending on the other terms in the Taylor expansion of f , are **Saddle-Node**, **Transcritical**, and **Pitchfork**.

The easiest model for the **Saddle-Node** is the differential equation:

$$\dot{x} = \mu - x^2$$

In this case two critical points exists for $\mu > 0$, one stable and one unstable. They collapse in a non-hyperbolic critical point when $\mu = 0$ and there are no critical points for $\mu < 0$.

The easiest model for the **Transcritical** is the differential equation:

$$\dot{x} = x\mu - x^2$$

In this case two critical points exists for any μ , one stable and one unstable. At $\mu = 0$ they interchange their stability.

The easiest model for the **Pitchfork** is the differential equation:

$$\dot{x} = x\mu - x^3$$

In this case three critical points exists for $\mu > 0$, one unstable and two stable. They collapse in a non-hyperbolic critical point when $\mu = 0$ and there is only one stable critical point for $\mu < 0$.

We will not study this bifurcations in our two models (1) and (4). Instead we will find the **Hopf Bifurcation**, a bifurcation which occurs in vector fields (5) with $n \geq 2$ $p \geq 1$. [2]

Consider system (5) with a parameter value μ_0 and equilibrium $x(\mu_0)$ at which $Df(, \mu_0)$ has a simple pair of pure imaginary eigenvalues, $\pm i\omega$, $\omega > 0$, and no other eigenvalues with zero real part. The implicit function theorem guarantees (since $Df(, \mu_0)$ is invertible) that for each μ near μ_0 there will be an equilibrium $x(\mu)$ near $x(\mu_0)$ which varies smoothly with μ . Nonetheless, the dimension of stable and unstable manifolds of $x(\mu)$ do change if the eigenvalues of $Df(x(\mu), \mu)$ cross the imaginary axis at μ_0 . This qualitative change in the local flow near $x(\mu)$ must be marked by some other local changes in the phase portraits not involving fixed points. The normal form theorem gives us the required information about how the generic problem differs from the system (5). By smooth changes of coordinates, the Taylor series of degree 3 for the general problem can be brought to the following form:

$$\begin{aligned} \dot{x} &= (d\mu + a(x^2 + y^2))x - (\omega + c\mu + b(x^2 + y^2))y, \\ \dot{y} &= (\omega + c\mu + b(x^2 + y^2))x + (d\mu + a(x^2 + y^2))y, \end{aligned} \quad (6)$$

which is expressed in polar coordinates as

$$\begin{aligned} \dot{r} &= (d\mu + ar^2)r, \\ \dot{\theta} &= (\omega + c\mu + br^2). \end{aligned} \quad (7)$$

Since the first equation in (7) is uncoupled, we see that there is a periodic orbit of (6) which is $r = \sqrt{\frac{-d\mu}{a}}$ if $\frac{-d\mu}{a} > 0$, obtained from the non-zero solution of $\dot{r} = 0$ in (7). If $a \neq 0$, $d \neq 0$ and $\frac{-d\mu}{a} > 0$ this solution exists. The content of Hopf bifurcation theorem is that the qualitative properties of (6) near the origin remain unchanged if higher-order terms are added to the system:

Theorem (Hopf). *Suppose that the system $\dot{x} = f(x, \mu)$, $x \in \mathbb{R}^n$, $\mu \in \mathbb{R}$ has an equilibrium (x_0, μ_0) at which the following properties are satisfied:*

- $D_x f(x_0, \mu_0)$ has a simple pure imaginary eigenvalues and no other eigenvalues with zero real part. Then there exists a smooth curve of equilibria $(x(\mu), \mu)$ with $x(\mu_0) = x_0$ and the eigenvalues $\lambda(\mu)$, $\bar{\lambda}(\mu)$ of $D_x f(x(\mu), \mu)$ which are imaginary at $\mu = \mu_0$ vary smoothly with μ .
- If moreover

$$\frac{d}{d\mu}(\Re(\lambda(\mu)))|_{\mu=\mu_0} = d \neq 0,$$

Then there is a unique three-dimensional center manifold passing through (x_0, μ_0) in $\mathbb{R}^n \times \mathbb{R}$ and a smooth system of coordinates (preserving the planes $\mu = \text{const.}$) for which the Taylor expansion of degree 3 of the center manifold is given by (6). If $a \neq 0$, there is a surface of periodic solutions in the center manifold which has quadratic tangency with the eigenspace of $\lambda(\mu_0)$, $\bar{\lambda}(\mu_0)$ agreeing to second order with the paraboloid $\mu = -(a/d)(x^2 + y^2)$. If $a < 0$, then these periodic solutions are stable limit cycles, while if $a > 0$, the periodic solutions are repelling.

In the case of a map $x_{n+1} = f(x_n, \mu)$, the simplest bifurcation of a fixed point occurs at $\mu = \mu_*$, when there is a fixed point $x_* = f(x_*, \mu_*)$ such that one eigenvalue λ_* of $Df(x_*, \mu_*)$ is $|\lambda_*| = 1$. The generic bifurcations for maps are **Saddle-Node** and **Period-doubling**. The Saddle-Node occurs when $\lambda_* = 1$, and the Period-doubling $\lambda_* = -1$.

The easiest model for **Saddle-Node** bifurcation is the map:

$$f(x, \mu) = x^2 + x - \mu$$

The bifurcation occurs when for certain value of parameter μ , $f'(x_*, \mu_*) = 1$. Again, as in the ODE case, two fixed points exists for $\mu > 0$, one stable and one unstable, and they collapse in a non-hyperbolic fixed point when $\mu = 0$ and there are no fixed points for $\mu < 0$.

A one-dimensional model for **Period-doubling** bifurcation is the map:

$$f(x, \mu) = \mu - x^2, \quad \mu > -\frac{1}{4}$$

This map undergoes a Saddle-Node bifurcation at $\mu = -\frac{1}{4}$, where two fixed points

$$x_1 = \frac{-1 + \sqrt{1 + 4\mu}}{2}, \quad x_2 = \frac{-1 - \sqrt{1 + 4\mu}}{2},$$

x_2 is stable and x_1 unstable, appear.

At $\mu = \frac{3}{4}$ the eigenvalue of the stable fix point x_2 becomes -1 . For a slightly bigger values of μ , x_2 loses its stability, and a period-2 stable orbit, appears.

2.6 Transition to chaos

Another phenomenon we will find in our models, is the **Period-doubling Cascade**. This occurs when there is a sequence μ_n such that for any μ_n there is a period-doubling bifurcation in the following way: at μ_1 a stable 2-periodic orbit appears. Then this 2-periodic orbit loses their stability at μ_2 , and a stable 4-periodic orbit appears. Then at μ_3 this 4-periodic orbit loses its stability and a new stable 8-periodic orbit appears and so on. Consequently at each μ_n a stable 2^n -periodic orbit is born.

Very often there is a scaling behaviour in the cascade of bifurcations. Feigenbaum noted that the ratios of parameter distance between two successive period-doubling approach a constant as the periods increase to infinity. Moreover, this constant is universal in the sense that it applies to a variety of dynamical systems. Specifically,

$$\lim_{n \rightarrow \infty} \frac{\mu_{n-1} - \mu_{n-2}}{\mu_n - \mu_{n-1}} = 4.669201609 \quad (8)$$

In many dynamical systems this cascade of bifurcations leads the system to a chaotic behaviour, and some times to the existence of an strange attractor. Next section is devoted to understand this concepts.

3 Chaos and Symbolic Dynamics

In this section we will show working with a classical example, the tools used to show that a system has chaotic behaviour. We will follow [4] and work with the quadratic family:

$$F_\mu(x) = \mu x(1 - x), \quad \mu > 1 \tag{9}$$

We will list some known properties about this map:

- It has two fixed points $p = 0$ and $p_\mu = \frac{\mu-1}{\mu}$.
- $0 < p_\mu < 1$
- If $x < 0$ or $x > 1$ then $F_\mu^n(x) \rightarrow -\infty$ as $n \rightarrow \infty$. Therefore the interesting dynamics occurs in the interval $I = [0, 1]$.
- If $1 < \mu < 3$:
 1. F_μ has an attracting fixed point at p_μ and a repelling fixed at 0.
 2. If $0 < x < 1$ then $F_\mu^n(x) \rightarrow p_\mu$ as $n \rightarrow \infty$.

Hence for $1 < \mu < 3$, F_μ has only two fixed points and all other points in I are asymptotic to p_μ . Thus the dynamics of F_μ are completely understood for μ in this range.

When μ passes through 3, the dynamics of F_μ becomes slightly more complicated: a new periodic point of period 2 is born. This is the beginning successive period doubling bifurcations as μ increases between 3 and 4, and this is an example of the bifurcation cascade we explained in the previous section. In fact for this concrete model the **Feigenbaum conjecture** is proved.

In the subject of Dynamical Systems I made a program to compute the first period-doubling bifurcation cascade, and to check the Feigenbaum asymptotic value. In the next table we write the obtained results. The parameter μ is the interval $[a_1, a_2]$ at the bifurcations,

```

a1=3.0000000000000000 a2=3.0000000000000001 periodo=2
a1=3.449489742783178 a2=3.449489742783179 periodo=4
a1=3.544090359551922 a2=3.544090359551923 periodo=8
a1=3.564407266095432 a2=3.564407266095433 periodo=16
a1=3.568759419543827 a2=3.568759419543827 periodo=32
a1=3.569691609801397 a2=3.569691609801398 periodo=64
a1=3.569891259378118 a2=3.569891259378119 periodo=128
a1=3.569934080000018 a2=3.569934080000018 periodo=256
a1=3.569943176048403 a2=3.569943176048404 periodo=512
a1=3.569945137342181 a2=3.569945137342182 periodo=1024
a1=3.569945557391250 a2=3.569945557391251 periodo=2048
a1=3.569945651200004 a2=3.569945651200005 periodo=4096
a1=3.569945674137600 a2=3.569945674137601 periodo=8192

```

a1=3.569945675202558 a2=3.569945675202558 periodo=16384
a1=3.569945675366397 a2=3.569945675366398 periodo=32768
a1=3.569945675402441 a2=3.569945675402442 periodo=65536

Next table shows the quotiens $\frac{\mu_{n-1}-\mu_{n-2}}{\mu_n-\mu_{n-1}}$ as they approach the Feigenbaum constant.

Constante Feigenbaum=4.656251017651319 Bifurcación periodo=16
Constante Feigenbaum=4.668242235577268 Bifurcación periodo=32
Constante Feigenbaum=4.668739469280134 Bifurcación periodo=64
Constante Feigenbaum=4.669132150837923 Bifurcación periodo=128
Constante Feigenbaum=4.662463268002508 Bifurcación periodo=256
Constante Feigenbaum=4.707607093391581 Bifurcación periodo=512
Constante Feigenbaum=4.637779656959092 Bifurcación periodo=1024
Constante Feigenbaum=4.669201579940650 Bifurcación periodo=2048
Constante Feigenbaum=4.477717195291651 Bifurcación periodo=4096
Constante Feigenbaum=4.089737763397038 Bifurcación periodo=8192
Constante Feigenbaum=21.538500512078038 Bifurcación periodo=16384
Constante Feigenbaum=6.500020328894406 Bifurcación periodo=32768
Constante Feigenbaum=4.545525109654527 Bifurcación periodo=65536

Now we focus on the dynamics when $\mu > 4$.

As before, all the interesting dynamics occur in the interval I . Note that, since $\mu > 4$ certain points of I leave I after one iteration of F_μ . We denote this set by A_0 , which is an open interval centered at $1/2$. All the other points in I remain in I after an iteration of the map.

Inductively, one can define

$$A_n = \{x \in I, F_\mu^n(x) \in A_0\}$$

That is

$$A_n = \{x \in I, F_\mu^i(x) \in I, F_\mu^{n+1}(x) \notin I\}$$

so that A_n consists in all the points which leave I at the $n + 1$ iteration of the map. Therefore, the only points which never escape from I are

$$\Lambda = I - \cup_{n \geq 0} A_n$$

Since A_0 is an open interval centered at $1/2$, then $I - A_0 = I_0 \cup I_1$, where I_0 and I_1 are two closed intervals and F_μ maps them to I . Now, if we consider $I - (A_0 \cup A_1) = I_{00} \cup I_{01} \cup I_{10} \cup I_{11}$ is the union of four closed intervals.

In general we have:

- A_n is the union of 2^n disjoint open intervals
- $I - A_0 \cup \dots \cup A_n$ is the union of 2^{n+1} closed intervals.
- F_μ^{n+1} maps each of the closed intervals to I , therefore the graph of F_μ^{n+1} has exactly 2^n bumps in I and therefore has 2^n fixed points. This implies that $Per_n(F_\mu) = 2^n$

- One can see that that Λ is a **Cantor set**, that is: it is closed, totally disconnected (does not contains intervals) and perfect (every point is an acumulation point of points in the set).
- Λ is a hyperbolic set, that is, for every $x \in \Lambda$ one has that $|F'_\mu(x)| > 1$.

It is clear that the structure of Λ is more complicated for $\mu > 4$.

3.1 Symbolic dynamics

Symbolic dynamics is a tool used to detect chaos in a dynamical system. We will show how it works in this unidimensional map. First we introduce an abstract dynamical system which will reflect the behaviour of the orbits in a chaotic system.

Consider the space

$$\Sigma_2 = \{s = (s_0 s_1 s_2 \dots), s_j = 0, 1\}$$

it is called the **sequence** space on the two symbols 0 and 1.

We can define a distance in the space as:

$$d(s, t) = \sum_{i \geq 0} \frac{|s_i - t_i|}{2^i}$$

which makes Σ_2 a metric space. Clearly, the distance between two sequences is smaller than $(1/2)^n$ if the first n entries are the same in both sequences. Then, two sequences are close provided their first few entries agree. We now define the most important ingredient in symbolic dynamics, the **Shift map** on Σ_2 :

$$\sigma : \Sigma_2 \rightarrow \Sigma_2$$

given by

$$\sigma(s_0 s_1 s_2 \dots) = (s_1 s_2 s_3 \dots)$$

The shift simply “forgets” the first entry of a sequence and shift the other one place to the left. Then, studying this simple map one can see:

- σ is continuous
- Let us note that the sequences formed by repeating a word of length n is a n -periodic point for σ , therefore

$$Per_n(\sigma) = 2^n$$

- $Per(\sigma)$ is dense in Σ_2 .
- There exist a dense orbit for σ in Σ_2 .

Now we will see that the shift map is an exact model for the quadratic map F_μ when $\mu > 4$.

3.2 Topological conjugacy

To see that the dynamic of our map F_μ in Λ is the “same” than the dynamics of σ in Σ_2 we have to build a conjugation between the two dynamical systems.

What we will do is to “follow” the orbit of a point and label it if its iterates are in the interval I_0 or I_1 . This sequence of numbers will give us the **itinerary** of the point x :

$$S(x) = (s_0 s_1 s_2 \dots), \text{ if } F_\mu^j(x) \in I_{s_j}$$

The itinerary of x is an infinite sequence of 0 and 1. That is, $S(x)$ is a point in the space Σ_2 . We think as S as a map from Λ to Σ_2 and we have that:

Theorem. *If $\mu > 2 + \sqrt{5}$ the $S : \Lambda \rightarrow \Sigma_2$ is an homeomorphism and $S \circ F_\mu = F_\mu \circ S$.*

As a consequence of this theorem we obtain a lot of information about F_μ in Λ :

1. The cardinality of $Per_n(F_\mu)$
2. $Per(F_\mu)$ is dense in Λ .
3. F_μ has a dense orbit in Λ

Finally there is another property the map F_μ verifies: it has **sensitive dependence with respect to initial conditions**

We say a map $f : M \rightarrow M$ has sensitive dependence with respect to initial conditions if there exists $\varepsilon_0 > 0$ such that $\forall x \in M, \forall \delta > 0$, there exists $k > 0, y \in M$ such that $d(x, y) < \delta$ and $d(f^k(x), f^k(y)) > \varepsilon_0$.

In fact, the dynamics of F_μ in Λ verifies the conditions of a **chaotic dynamical system**:

- Periodic orbits are dense: every orbit in the space is approached arbitrarily closely by periodic orbits
- There exists a point whose orbit is dense
- It has sensitive dependence with respect to initial conditions.

For more general dynamical systems, a useful tool to understand their dynamics, mainly the existence of periodic orbits and transitivity property, are **transition graphs**.

Assume we have a map $f : I \rightarrow I, I \subset \mathbb{R}$ and a set of disjoint intervals $I_0, I_1, \dots, I_n, I_j \subset I$. An arrow is drawn from I_j to I_k in a **transition graph** if and only if the image $f(I_j)$ contains the subinterval I_k .

For instance a transition map for the logistic studied in this section is given by **Figure 1**.

In topological dynamics of interval maps the main tool is the following straightforward consequence of *Bolzano's Theorem*:

Theorem (Fixed-Point). *Let f be a continuous map of the real line, and let $I = [a, b]$ be an interval such that $f(I) \supset I$. Then f has a fixed point in I .*

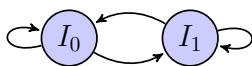


Figure 1: Transition graph for the logistic map

Several consequences of this theorem can be stated using transition graphs. For instance, if the graph contains $I_j \rightarrow I_j$, the map has a fixed point in I_j . If the graph contains a pair of intervals $I_k \rightarrow I_l \rightarrow I_k$, then $f^2(I_k) \supset I_k$ and then there is a two periodic point of f in I_k . In general, if the graph contains $I_{i_1} \rightarrow I_{i_2} \rightarrow \dots \rightarrow I_{i_n} \rightarrow I_{i_1}$, the map f has a n -periodic point in I_{i_1} .

The more spectacular result is consequence of combining these tools with **Sharkovskii Theorem**.

Sharkovskii gave a scheme for ordering the natural numbers in an unusual way so that for each natural number n , the existence of a period- n point implies the existence of periodic orbits of all the periods higher in the ordering than n . Here is Sharkovskii's ordering:

$$3 \prec 5 \prec 7 \prec 9 \prec \dots \prec 2 \cdot 3 \prec 2 \cdot 5 \prec \dots \prec 2^2 \cdot 3 \prec 2^2 \cdot 5 \prec \dots \\ \dots \prec 2^3 \cdot 3 \prec 2^3 \cdot 5 \prec \dots \prec 2^4 \cdot 3 \prec 2^4 \cdot 5 \prec \dots \prec 2^3 \prec 2^2 \prec 2 \prec 1.$$

Theorem (Sharkovskii). *Assume that f is a continuous map on an interval and has a period p orbit. If $p \prec q$, then f has a period- q orbit.*

A easy consequence of this theorem is that if a map has a period-3 orbit then it has orbits of any period. Therefore, if our transition graph contains three intervals $I_{i_1} \rightarrow I_{i_2} \rightarrow I_{i_3} \rightarrow I_{i_1}$ the map has a period-3 point, and therefore it has points of any period.

In fact, once we have a transition graph in I_0, \dots, I_n for a map f , one can make an analogous construction as the one we have done for the logistic map. We consider the space of sequences Σ_n of $n + 1$ symbols and the shift map in it. The transition graph of f will tell us which sequences are admissible in Σ_n . To label which sequences are admissible, one usually uses the so called **transition matrix**, a $n + 1$ square dimensional matrix where the entry a_{ij} is 1 if the transition graph contains an arrow from I_i to I_j , and a zero otherwise.

It is a known result that if A^k has no zero entries for some k the system has chaos.

3.3 Strange attractor

In general dynamical systems there are attractor sets which have a complicated structure. The main idea of an attractor, is an attracting set such that the dynamics in it is chaotic. There exist different definitions in mathematical literature of strange attractors. Here we put the definition of strange attractor given in [1, 4] for a map f .

Given a map $f : M \rightarrow M$, we call an invariant set $S \in M$ a chaotic strange attractor if:

- S Is an attractor.

- There exists a point in S whose orbit is dense in S .
- it has sensitive dependence with respect to initial conditions.

There are other definitions of strange attractors. One of them is based in the concept of **Lyapunov Exponents**.

3.3.1 Lyapunov Exponents

For a one-dimensional map f , following [7], we define the **Lyapunov Exponent** of an orbit $\{x_1, x_2, x_3, \dots\}$, where $x_i = f^{i-1}(x_1)$ as:

$$h(x_1) = \lim_{n \rightarrow \infty} \frac{\ln |f'(x_1)| + \dots + \ln |f'(x_n)|}{n}.$$

There exist analogous definitions in higher dimension of Lyapunov Exponents, and some authors like [7] ask the chaotic strange attractors to have positive Lyapunov exponent.

Other definitions of strange attractors need the concept of **Fractal dimension**.

3.3.2 Fractal Dimension

There are several definitions of the fractal dimension. For practical purposes, the most used is the box-counting dimension and is explained in [7].

The idea of the box-counting dimension of a set S in a m -dimensional space, is to count how many m -dimensional boxes of side-length ε does it take to cover the object S . For objects in three-dimensional space, we cover with cubes of side ε . The idea is that an object will have dimension d if the number of boxes we need is of order $(1/\varepsilon)^d$, for small ε . In general, if S is a set in \mathbb{R}^m , we would like to say that S is a d -dimensional set when it can be covered by $N(\varepsilon) = C(1/\varepsilon)^d$ boxes of side-length ε , for small ε . In this way, it is not required that the exponent d be an integer.

Let S be a bounded set in \mathbb{R}^m . To measure the dimension of S , we lay a grid of m -dimensional boxes of side-length ε over S . Set $N(\varepsilon)$ equal to the number of boxes of the grid that intersect S . Solving the scaling law for the

dimension d gives us

$$d = \frac{\ln N(\varepsilon) - \ln C}{\ln(1/\varepsilon)}.$$

If C is constant for all small ε , the contribution of the second term in the numerator of this formula will be negligible for small ε . This justifies the following definition:

A bounded set S in \mathbb{R}^n has **box-counting dimension**

$$\text{Boxdim}(S) = \lim_{\varepsilon \rightarrow 0} \frac{\ln N(\varepsilon)}{\ln(1/\varepsilon)}$$

when the limit exists.

4 Numerical Methods

In this work we have studied two real models given by three dimensional equations that can not be treated analytically. Therefore, we have combined the theoretical knowledge of Dynamical systems with some numerical methods to understand the dynamics and mainly the asymptotic behaviour of the solutions.

The first tool needed to find these solutions is a good numerical integrator for ordinary differential equations.

4.1 Numerical Integrators of odes

Here we will consider the initial value problem:

$$y' = f(t, y), \quad y(t_0) = y_0. \quad (10)$$

4.1.1 Runge-kutta

The (possibly) most used method to integrate an ode is the classical fourth-order Runge-kutta method.

The Runge-kutta method for an initial value problem (10), gives the values of the solution $y_n = y(t_n)$, with $t_n = t_0 + nh$ and h is the step of the method as:

$$y_{n+1} = y_n + \frac{1}{6} (k_1 + 2k_2 + 2k_3 + k_4)$$

$$t_{n+1} = t_n + h$$

$$k_1 = hf(t_n, y_n),$$

$$k_2 = hf(t_n + \frac{1}{2}h, y_n + \frac{1}{2}k_1),$$

$$k_3 = hf(t_n + \frac{1}{2}h, y_n + \frac{1}{2}k_2),$$

$$k_4 = hf(t_n + h, y_n + k_3).$$

Thus, the next value (y_{n+1}) is determined by the present value (y_n) plus the weighted average of four increments, where each increment is the product of the size of the interval, h , and an estimated slope specified by function f on the right-hand side of the differential equation.

Even if this is a good numerical integrator, the local error at each step is of order $O(h^5)$ and the global error is of order $O(h^4)$, it is not very fast. The classical way to improve the accuracy is to use a variable step size using step size control. As we will deal with a chaotic regime (we are interested in finding a chaotic attractor) the sensitive dependence respect to initial conditions obliges the step size to be very small to do not loose accuracy. This makes the method too slow to study the asymptotic behaviour of the system when it has chaotic behaviour and strange attractors.

4.1.2 The Taylor method

A way to produce numerical integrators of very high order is by means of Taylor expansions. Most of the books in Numerical Analysis in the literature disregarded these methods

because, to apply it, one has to find high order derivatives, and this is “supposedly” difficult. In Stoer Bulsh book [?] page 414-415, it is said: “The higher-order methods so obtained, however are hardly useful, since in every step $(x_i, \eta_i) \rightarrow (x_{i+1}, \eta_{i+1})$, one must compute not only f (the vector field), but also the partial derivatives f_x, f_y , etc.

Nevertheless the dynamical system group in the UB has experts that have developed a systematic and programmable way to compute this derivative: the so called **automatic differentiation**. This makes this method very powerful.

A very good explanation of this method can be found in [6]

Again we will consider the initial value problem (10). The main idea of this method is to write the unknown $y(t)$ in a Taylor series around t_n up to order N :

$$\begin{aligned} y(t) &= a_0 + a_1(t - t_n) + \dots + a_N(t - t_n)^N \\ y'(t) &= a_1 + 2a_2(t - t_n) + \dots + Na_N(t - t_n)^{N-1} + (N + 1)a_{N+1}(t - t_n)^N \end{aligned}$$

then one can also write the Taylor expansion up to of the right hand side of the equation up to order N

$$f(t, y(t)) = b_0 + b_1(t - t_n) + \dots + b_N(t - t_n)^N$$

and these coefficients only depend on a_1, \dots, a_N . Then, the differential equation becomes:

$$a_1 + 2a_2(t - t_n) + \dots + Na_N(t - t_n)^{N-1} + (N + 1)a_{N+1}(t - t_n)^N = b_0 + b_1(t - t_n) + \dots + b_N(t - t_n)^N$$

and from this last equation we can find $a_{N+1} = b_N / (N + 1)$.

When one uses a numerical integrator in a ordinary differential equation, one important point is the step size. The bigger the step the faster the method. The reason is clear, the number of computations decreases as the size of the step increases. But we need to make the optimal choice of the step size to perform the minimum number of computations with the accuracy we want to obtain.

Therefore we need to control the maximum value the step $h = (t_{n+1} - t_n)$ can achieve.

In [5] it is shown how to choose in an optimal way, the step size h and the order of truncation of the Taylor series p to obtain a given accuracy ε and minimize the number of computations per unit of time.

- A straightforward choice to ensure a good accuracy is

$$h = \rho \left(\frac{\varepsilon}{M} \right)^{\frac{1}{p+1}}, \quad (11)$$

where ρ is an approximated value of the convergence ratio of convergence of the Taylor series and p is the order of truncation.

- One can see that the number of computations for unit of time is approximately given by

$$\phi(p) = \frac{c(p + 1)^2}{\rho \left(\frac{\varepsilon}{M} \right)^{\frac{1}{p+1}}}.$$

- Minimizing the function ϕ one gets the optimal truncation value as:

$$p = -\frac{1}{2} \ln\left(\frac{\varepsilon}{M}\right) - 1$$

- Once we have the optimal value of p we obtain h from (11):

$$h_{max} = \rho/e^2$$

The estimate of ρ is obtained by estimating $|a_n|^{-1/n}$ for $n = p - 2, p - 1, p$.

This method has advantages respect to the Runge-Kutta one: mainly when we are in a part of the phase space where the solution has a big radius of convergence, because this allows us to use big step size without losing accuracy getting a fast method. For this reason, in this work, we will use always this method.

4.2 Other standard numerical tools

In this section we briefly describe some complementary numerical tools we have used to analyse our models (4) and (1): the numerical differentiation and extrapolation and some methods for looking for zeros of a map.

4.2.1 Zero finders

In this work we use four different methods to look for zeros of different one and two dimensional functions: **the iteration method**, **bisection method**, **Secant method** and **Newton method**. Each one has advantages and disadvantages depending of the map, so we will use one or another in different situations of our work. We will have a function:

$$F : \mathbb{R}^n \rightarrow \mathbb{R}^n$$

and we look for $\alpha \in \mathbb{R}^n$ such that

$$F(\alpha) = 0 \tag{12}$$

An important issue in these kind of problems is to begin the iteration at a point x_0 such that $|x_0 - \alpha|$ is small enough. This will make the method work faster and, moreover, will ensure that our method converges to the suitable root α we are looking for, when the function F has several zeros. As our function will be the Poincaré map of an autonomous vector field depending on parameters we will use the Theorem of continuous (and differentiable) dependence of solutions with respect to initial conditions and parameters. This will allows us to use a continuation method with respect to parameters. After a small variation of the parameter, we will use as the new initial condition the just computed zero of the function for a value of the parameter nearby.

Sometimes, it will be enough to use the **Iteration method**, which, consists in building a sequence $X_{n+1} = G(X_n)$, for $G = F + Id$. If $G : B \rightarrow B$ is a contraction ($|DG(x)| < 1$, $\forall x \in B$) one can apply the fix theorem to the function G and this sequence will converge to the fix point of the function G .

A very straightforward method for one-dimensional maps, that simply relies in Bolzano's theorem is the **Bisection method**. One needs to find two values a and b with $F(a)F(b) < 0$ and then build a sequence of intervals

$$(a, b) = (a_0, b_0) \supset (a_1, b_1) \supset \dots \supset (a_k, b_k) \supset \dots,$$

We choose (a_{k+1}, b_{k+1}) from (a_k, b_k) , considering $c_k = (a_k + b_k)/2$. Then we choose the new interval (a_k, c) or (c, b_k) depending on $F(a_k) \cdot F(c) < 0$ or $F(c) \cdot F(b_k) < 0$ respectively.

This is a very slow method but its advantage is that is always convergent. We will often use this method as a first step to get a reasonable approximated value of the root and then apply a fast method, like the Newton method, to improve its accuracy.

If we are dealing a one dimensional map and computing the derivative is very expensive one can use as an alternative the **Secant method**. As it is known the Newton method approximates the zero of the function F by the zero of the tangent line to F at the point x_k . The secant method instead approximates it by the zero of the secant line to F at the point x_k and x_{k-1} .

$$x_{k+1} = x_k - f(x_k) \frac{x_k - x_{k-1}}{f(x_k) - f(x_{k-1})} \quad (k \geq 1).$$

The **Newton method** is one of the most used methods to find zeroes of functions due to its fast convergence, but it only can be used if one has a good enough approximation X_0 of the root. The method gives us a sequence:

$$X_{k+1} = X_k - (DF(X_k))^{-1}F(X_k) \tag{13}$$

wich converges to a zero α of F and can be used in any dimension. To use this method one needs to know the derivatives of the function F . We will use the Newton method several times in our work. First to compute the time where our solutions intersect a given section when computing the corresponding Poincaré map. Later to look for fixed or periodic points of this map. In both cases we will not have analytic expressions of the map F whose zero we are looking for. Then we need a numerical method to compute the derivatives of F . This can be numerically expensive because the discretized formulas for the derivatives are numerically unstable (they always are given by quotients of quantities which are close to zero). On the other hand we know that Newton method has quadratic convergence if the Jacobian matrix is not singular or close to singular.

In case we are dealing with a n-dimensional system we will not compute DF^{-1} in formula (13). Instead we will solve the linear system

$$DF(X_k)\Delta = -F(X_k)$$

And then

$$X_{k+1} = X_k + \Delta.$$

We proceed in this way because to compute the inverse are as expensive as solving n linear systems.

4.2.2 Numerical Differentiation

To numerically compute the derivative of a function f the simplest method is just to use its definition

$$f'(x) = \frac{f(x+h) - f(x)}{h} + O(h)$$

or even better

$$f'(x) = \frac{f(x-h) - f(x+h)}{2h} + O(h^2) = D(h) + a_2h^2 + a_4h^4 + \dots \quad (14)$$

The formulas above are quite delicate, numerically speaking: subtracting similar quantities and quotients by small quantities are a source of lose significant digits and accuracy. Then we can not choose a very small values of h , to get small error of the approximations formulas above. Instead we will use extrapolation.

The **extrapolation method** is a method used to improve approximated formulas, when one can compute the approximated formula, which has an error of order $O(h^k)$, with different values of the step size h . The method also allows to estimate the constants in the asymptotic formulas of the error.

Let $A(h)$ be an approximation of A that depends on a positive step size h with an error formula of the form:

$$A - A(h) = ah^k + O(h^{k'}) \quad k' > k$$

Using two different step size h and h/t we have:

$$\begin{aligned} A &= A(h) + ah^k + O(h^{k'}) \\ A &= A(h/t) + a(h/t)^k + O(h^{k'}) \end{aligned} \quad (15)$$

Then multiplying the second equation by t^k and subtracting the first equation gives

$$(t^k - 1)A = t^k A(h/t) - A(h) + O(h^{k'})$$

Hence,

$$A = \frac{t^k A(h/t) - A(h)}{(t^k - 1)} + O(h^{k'})$$

Which is a better approximation of the expression A .

This process can be repeated to remove more error terms to get even better approximations, this is called the repited Richardson extrapolation.

We can also obtain the value of the first asymptotic constant of the error: subtracting the second equation in (15) to the first one one can obtain the constant a :

$$a \simeq \frac{A(h/t) - A(h)}{h^k(1 - 1/t^k)}.$$

When applying one step of extrapolation to the formula (14) one obtains:

$$\frac{4D(h/2) - D(h)}{3}$$

5 Analysis of the Models

As we said in section 1 in this work we will study two ecological models: The three-species food chain (1), and the epidemic model SEIR (4).

From the ecological point of view, the main purpose when one studies these models, is to be able to make predictions and understand the past the present and future behaviour of the system. Consequently it is fundamental to obtain and understand the attractors of the system. These sets are the ones where the systems would be with highest probability. Moreover, the solutions of the system will approach this sets in natural way. Furthermore, these are the sets which can easily be obtained numerically. Therefore our main purpose would be how these sets behave when a parameter of the system vary between two valid ecological values. We will focus on the food-chain model, and we will give a detailed explanation of this model, but the general scenario is very similar for SEIR model.

We begin by sweeping the parameter space to detect the different qualitative behaviour. Lately we will focus on each qualitative different region.

In the three-specie model (1) we will fix all the parameters except $b_1 \in [2, 6.2]$. This parameter is related to the interaction between the species X and Y . We will see that different values of b_1 gives rise to different qualitative behaviour of the system.

One general fact is that the planes $x = 0$, $y = 0$, $z = 0$ are invariant planes. This is a consequence of the fact that normal vectors to these surfaces $((1, 0, 0), (0, 1, 0), (0, 0, 1))$ are orthogonal to the vector field. As consequence the region

$$\{(x, y, z), x \geq 0, y \geq 0, z \geq 0\}$$

is an invariant region. In fact, it has no sense to study regions of the phase space with negative values of the variables because those have no biological meaning. Therefore, during this work we have restrict ourselves to the positive region.

5.1 Local behaviour

The system has in general 6 equilibrium points $p_1 \dots p_6$ given by:

$$\begin{aligned} p_1 &= \left(0, \frac{d_2}{a_2 - b_2 d_2}, -\frac{d_1}{a_2 - b_2 d_2}\right) \\ p_2 &= (1, 0, 0) \\ p_3 &= \left(\frac{d_1}{a_1 - b_1 d_2}, \frac{a_1 - (1 + b_1)d_1}{(a_1 - b_1 d_1)^2}, 0\right) \\ p_4 &= (x_4, y_4, z_4) \\ p_5 &= (x_5, y_5, z_5) \\ p_6 &= (0, 0, 0) \end{aligned}$$

where

$$\begin{aligned}
x_4 &= \frac{(1+b_1)a_2 + (1-b_1)b_2d_2 - \sqrt{(a_2 - b_2d_2)((1+b_1)^2a_2 - (4a_1b_1 + (1+b_1)^2b_2)d_2)}}{2b_1(a_2 - b_2d_2)} \\
y_4 &= \frac{d_2}{a_2 - b_2d_2} \\
z_4 &= \frac{(1+b_1)(a_1 - b_2d_2) - 2a_1b_1d_2 + 2b_1^2d_1d_2 + \sqrt{(a_2 - b_2d_2)((1+b_1)^2a_2 - (4a_1b_1 + (1+b_1)^2b_2)d_2)}}{2b_1^2d_2(b_2d_2 - a_2)} \\
x_5 &= \frac{(b_1 - 1)a_2 + (1 - b_1)b_2d_2 + \sqrt{(a_2 - b_2d_2)((1+b_1)^2a_2 - (4a_1b_1 + (1+b_1)^2b_2)d_2)}}{2b_1(a_2 - b_2d_2)} \\
y_4 &= \frac{d_2}{a_2 - b_2d_2} \\
z_4 &= \frac{(1+b_1)(b_2d_2 - a_2) + 2a_1b_1d_2 - 2b_1^2d_1d_2 + \sqrt{(a_2 - b_2d_2)((1+b_1)^2a_2 - (4a_1b_1 + (1+b_1)^2b_2)d_2)}}{2b_1^2d_2(a_2 - b_2d_2)}
\end{aligned}$$

We recall that we will take the values of the parameters as

$$a_1 = 5, \quad a_2 = 0.1, \quad b_2 = 2, \quad d_1 = 0.4, \quad d_2 = 0.01 \quad (16)$$

We have written a code which computes the points and the Jacobian J of the vector field at them. Then using the direct or inverse power iteration method, the fact that $\lambda_1\lambda_2\lambda_3 = \det(J)$ and $\lambda_1 + \lambda_2 + \lambda_3 = \text{tr}(J)$ we have computed the eigenvalues for different values of the parameter b_1 . In this way we have obtained:

- p_1 does not vary with b_1 , but is not in the positive region and therefore we will not consider it.
- The point p_2 does not vary with b_1 . It is always a saddle with two negative eigenvalues and a positive one. For instance when $b_1 = 2$ they are: $\lambda_1 = 1.266667$, $\lambda_2 = -0.01$, $\lambda_3 = -1$.
- The point p_3 is in the positive region. It is an unstable focus with two complex eigenvalues with positive real part, and a positive real one. For instance when $b_1 = 2$ the point is $(0.095238, 0.215420, 0)$ and the eigenvalues are: $\lambda_1 = 0.005237$, $\lambda_2 = 0.030913 + 0.544651i$, $\lambda_3 = 0.030913 - 0.544651i$.
- p_4 is not in the positive region, therefore we will not consider it.
- The point p_5 is in the positive region. It is an stable focus with two complex eigenvalues with negative real part, and a real negative one. At $b_1 = 2.1$ the point is $(0.759062, 0.125000, 13.288677)$, and the eigenvalues are: $\lambda_1 = -0.395013$, $\lambda_2 = -0.001687 + 0.114683i$, $\lambda_3 = -0.001687 - 0.114683i$. See **Figure 2**

After $b_1 = 2.1$ the point p_5 undergoes a *Hopf Bifurcation* becoming a saddle-focus with two complex eigenvalues with positive real part, and a real negative one. At

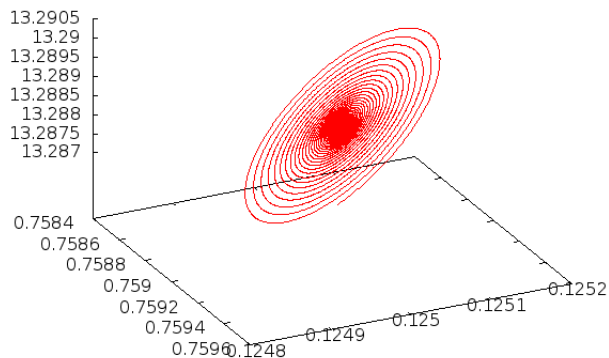


Figure 2: Stable focus at $b_1 = 2.1$ before Hopf bifurcation

this Hopf bifurcation a stable periodic orbit γ , of size $O(\sqrt{b_1 - b_1^*})$ is born around it, where b_1^* is the bifurcation value. For instance at $b_1 = 2.2$ the eigenvalues are: $\lambda_1 = -0.434119$, $\lambda_2 = 0.009033 + 0.108102i$, $\lambda_3 = 0.009033 - 0.108102i$. See **Figure 3**

As we will see, this bifurcation is the origin of the transition to chaos through a *period-doubling cascade* of the periodic orbit γ .

- The point p_6 does not vary, and it is always a saddle with two negatives eigenvalues, and a positive one.

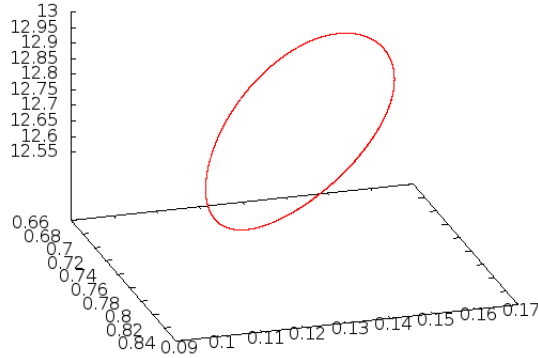


Figure 3: Stable periodic orbit at $b_1 = 2.2$ after Hopf bifurcation

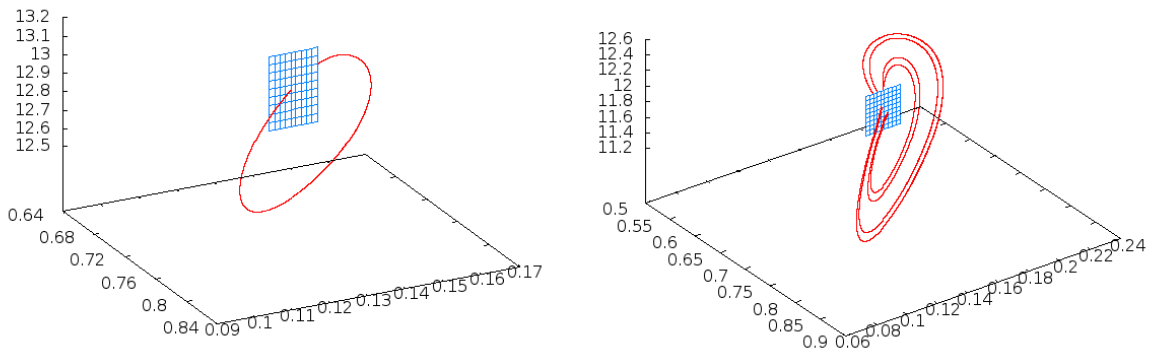


Figure 4: Poincaré section at $x = 0.75$ for periodic orbit at $b_1 = 2.2$ and at $b_1 = 2.3839$

5.2 Transition to chaos

In this section we will show how the Hopf bifurcations experienced by the point p_5 , is the beginning of a set of bifurcation which will lead the system to a chaotic behaviour and the birth of the strange attractor.

As we explained in the previous section at $b_1 = b_1^*$ a periodic orbit γ appears around p_5 . To study the behaviour of γ when varying b_1 , and also the behaviour of the orbits near γ , we will use the *Poincaré map*. By numerical observations we decided to take as a good Poincaré section (see **Figure 4**):

$$\Sigma = \{(x, y, z), x = x^*\} \quad x^* = 0.75$$

To compute the Poincaré map, we have taken a point $p_0 \in \Sigma$, and we have built the solution $\phi(t, p_0)$ using the *Taylor method* until it reaches again Σ with the same orientation. To have an accurate approximation of $P(p_0)$ we need to have an accurate

approximation of the time $t_0 > 0$ such that $\phi(t_0, p_0) \in \Sigma$. To obtain t_0 we have proceeded in two steps:

1. We have extend the solution until a time t such that

$$(\pi_x \phi(t, p_0) - x^*)(\pi_x \phi(t + h, p_0) - x^*) < 0,$$

where h step in the Taylor method.

2. Taking either $t_0 = t$ or $t_0 = t + h$, we improve the value of the crossing time t_0 by applying the *Newton method* to solve the equation

$$\pi_x(\phi(t + h, p_0) - x^*) = 0.$$

As ϕ is the solution of the ODE (1), we can get the derivative in terms of ϕ :

$$\pi_x(\phi)' = \pi_x(\phi)(1 - \pi_x(\phi)) - f_1(\pi_x(\phi))\pi_y(\phi)$$

Obviously, $p^* = \gamma \cap \Sigma$ is a fixed point of the Poincaré map. If γ is a stable periodic orbit, the point p^* is a stable fixed point of the Poincaré map. Nevertheless, as we want to detect the bifurcations we need a numerical method to compute the eigenvalues of $DP(p^*)$. We use the numerical differentiation and extrapolation explained in section 4.2. For instance for $b_1 = 2.2$ the point is

$$p^* = (0.127731729624708, 12.996965239079815)$$

and the eigenvalues are

$$\lambda_1 = -0.000000263444777 \quad \lambda_2 = -0.066970693318373$$

Next step is to find several period-doubling bifurcations of the periodic orbit γ . As we will work with the Poincaré map, we will look for values of b_1 such that one of the eigenvalues of $DP(p^*)$ becomes -1 , in fact it will be λ_2 .

To get this value of b_1 we proceed as follows:

- Increase $b_1 = b_1 + \Delta b_1$.
- Compute the new fixed point iterating the map.
 1. If we are far away from bifurcations these iterates converge fastly to the new fixed point.
 2. If we approach the bifurcation value, as the fixed point loses stability, the iterates do not converge to the new fixed point. Therefore what we do is to apply Newton method, to get it.
- We compute the eigenvalues of de Jacobian of the Poincaré map, that in this case will have modulus less than 1.

When λ_2 crosses the value -1 , we have already passed the bifurcation value, b_1^1 where the period-doubling occurs. To improve the accuracy of the value we apply the *Secant method* to solve the equation

$$1 + \text{tr}(J(b_1)) + \det(J(b_1)) = 0$$

using the secant method.

Obviously at every step of the secant method, we have to find the fixed point of P , by combining iteration and Newton.

Proceeding in this way, we have obtained the first period-doubling bifurcation value at $b_1 \simeq 2.290883230232997$. In **Figure 6** we show the two periodic orbit which arises at this bifurcation.

We find the next period-doubling bifurcations applying the same methodology to the maps P^2 , P^4 , etc. In this way we have found the following bifurcation values:

- $b_1 = 2.290883227570100$ period 2
- $b_1 = 2.378002203462342$ period 4
- $b_1 = 2.390795195220854$ period 8
- $b_1 = 2.393734238320441$ period 16
- $b_1 = 2.393800222850270$ period 32

The previous method has been designed to get a quantitative and accurate information of the successive bifurcation values, nevertheless there is a faster way to realise that this bifurcations take place. We plot the classical bifurcation diagram: in the x -axis we plot the parameter b_1 and in the y -axis we plot the second component of the stable periodic point, obtained after a large number of iteration of the Poincaré map. To avoid the transition behaviour we do not plot the points until we get around 15000 units of time in the integration process. One can see this bifurcation diagrams in **Figure 5**. Looking at this figure one can also see that after the period-doubling cascade we have studied, other period-doubling cascades occur. For instance as b_1 decreases approximately from 2.55 to 2.45 there is a period-doubling cascade that seems to meet with the first one. In the picture also appear other cascades beginning with a different period.

Looking at the bifurcation diagram, it seems to appear a bifurcation cascade which ends in an strange attractor at $b_1 = 3$. Moreover, integrating the system for near values the set of periodic orbits seems to have the shape of the strange attractor that appears after this (last?) bifurcation cascade (see **Figure ??**).

Finally we have computed the Feigenbaum constant using its definition (8) and the best result computed is: 4.670999

That is not so accurate value as in the logistic case, but in this case the problem is quite more difficult, because in this case the solution have to be numerically integrated. In addition, as we will explain later, the Jacobian matrix is ill-conditioned because it has a eigenvalue very close to zero and also all bifurcations are closer to each other than in the logistic case, making the significant digits to be out of our precision control.

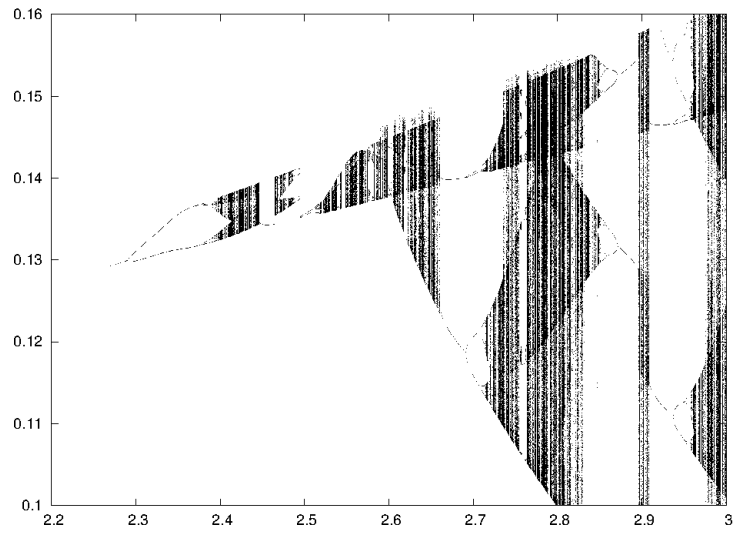


Figure 5: Bifurcation diagram for Poincaré map (plotting y)

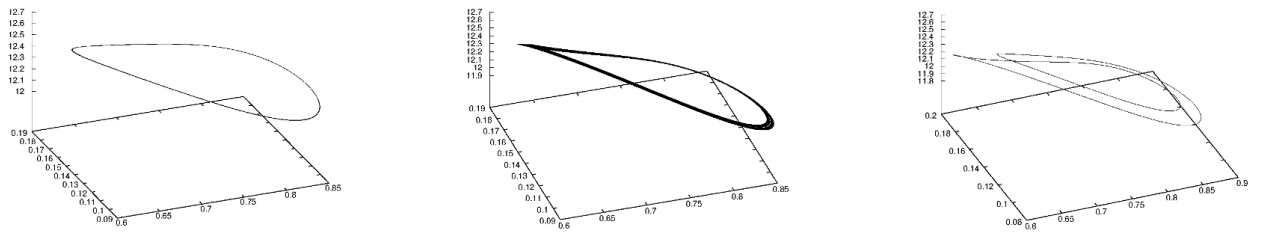


Figure 6: First period-doubling bifurcation, $b_1 = 2.28$, $b_1 = 2.29$, $b_1 = 2.3$

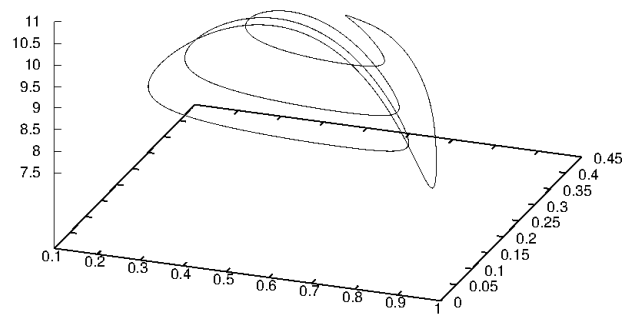


Figure 7: Periodic orbit corresponding to a 3-periodic point of the Poincaré map ($b_1 = 2.93$)

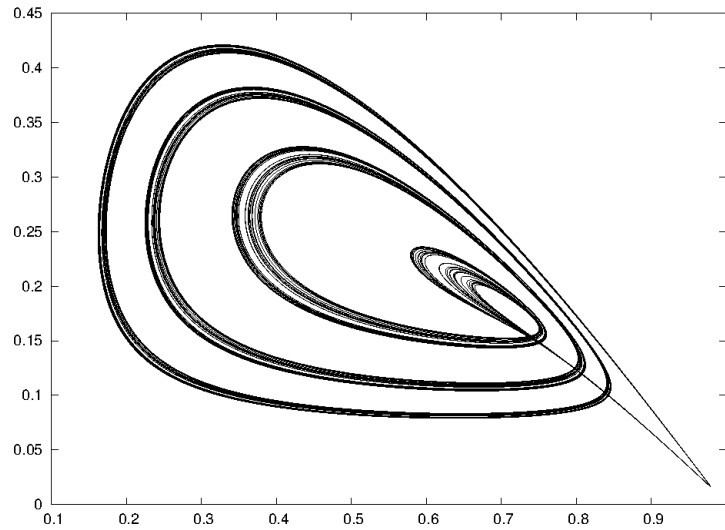


Figure 8: High-periodic orbit takes the shape of Strange Attractor ($b_1 = 2.96$)

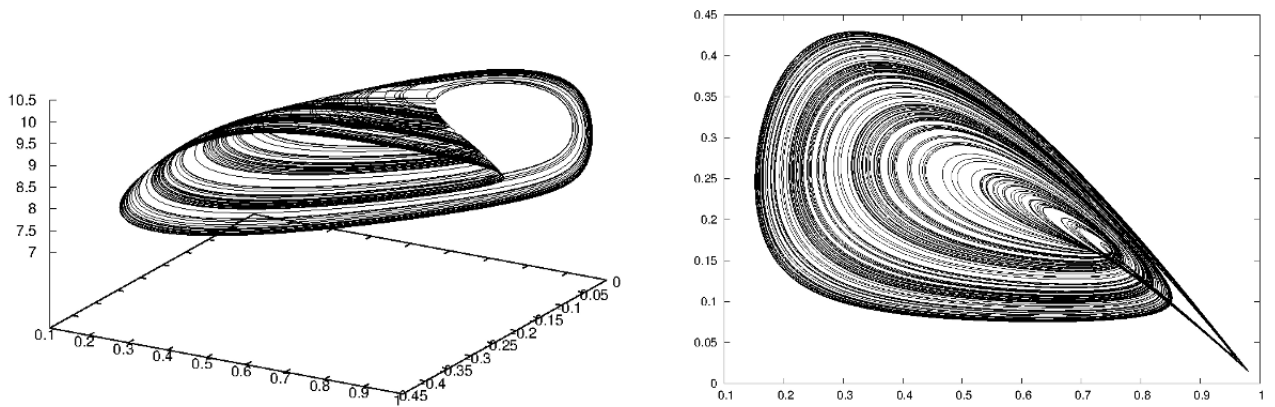


Figure 9: Strange attractor

5.3 Strange Attractor

In this section we will numerical study the Strange Attractor the system has for $b_1 = 3$ after the period doubling cascades. The global analysis of a strange attractor is quite difficult. Even to have rigorous evidences of its existence is quite complicated due to the fact that it is easy to confuse it with a set of periodic orbits (of very high period). Moreover, to deal with a three dimensional system makes the graphic analysis very difficult. Therefore we will use some known techniques which allow us to find insides working with a one dimensional map: the so called *transition graphs*. The results obtained studying this one dimensional system can be translated to understand phenomena which occur in the real three dimensional Dynamical System we are studying.

A first reduction of the dimension of the system can be done by considering again a suitable Poincaré map. After numerical observations it seems convenient to choose a

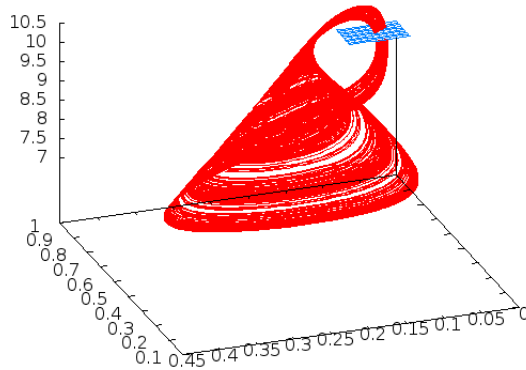


Figure 10: Poincaré section at $z = 9.3$ at $b_1 = 3.0$

Poincaré section (see **Figure 10**):

$$\Sigma = \{(x, y, z), z = 9.3\}$$

The results of this map are in **Figure 11**

Looking at **Figure 10** one can see that the Poincaré map is very contracting in one dimension, that is, one of the eigenvalues of its Jacobian is very close to zero. This has been a difficulty in applying the different methods because the derivative of P is close to singular. One can check this fact the well-known formula ([9]):

$$\det DP(\gamma(0)) = e^{\int_0^T \operatorname{div} X(\gamma(t)) dt}$$

On the other hand, this property makes this Poincaré map very suitable to be studied using the methodology for one-dimensional maps called transition graph.

Now, to get a transition graph for this map, we proceed as follows:

If our Poincaré map P sends the point (x_n, y_n) to the point (x_{n+1}, y_{n+1}) we define the map f as the one dimensional map such that $f(x_n) = x_{n+1}$ and we plot the graphic of the map f . A plot of this map is given in figure **Figure 12**. Looking at this figure one can observe the following facts:

- $f : I \rightarrow I$, $I = [0.946, 0.975]$
- We choose a partition of $I = I_1 \cup I_2 \cup I_3$, with $I_1 = [0.946, 0.957]$, $I_2 = [0.957, 0.963]$, $I_3 = [0.963, 0.975]$, and their transition graph is given in **Figure 13** (see also **Figure 12**)
- The transition matrix for this graph is:

$$M = \begin{pmatrix} 0 & 0 & 1 \\ 1 & 1 & 0 \\ 1 & 1 & 1 \end{pmatrix}$$

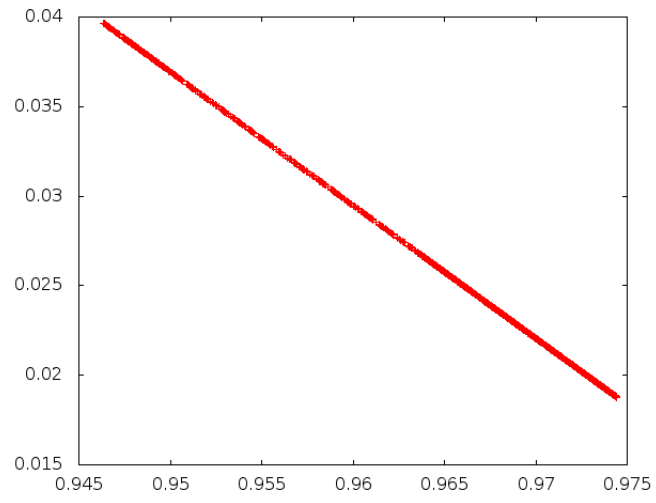


Figure 11: Poincaré map (section at $z = 9.3$ at $b_1 = 3.0$)

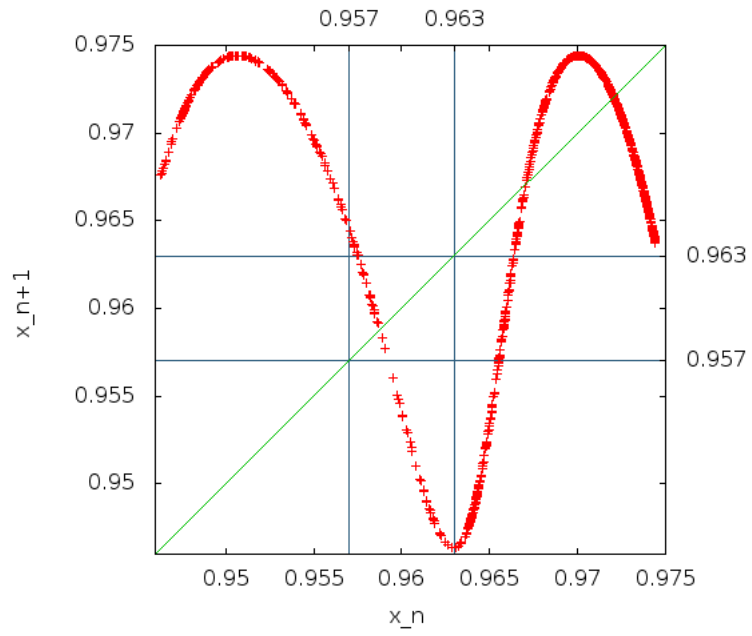


Figure 12: Poincaré map $x_{n+1} = P(x_n)$

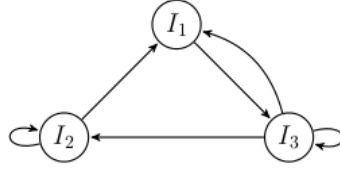


Figure 13: Transition graph for Poincaré map $x_{n+1} = P(x_n)$

As a consequence we know:

1. There is a fixed point of f in I_2 and another in I_3 (see **Figure 12**. Later we will choose a new set of smaller intervals that will give us extra information.
2. There is a two periodic orbit in I_1 whose orbit moves between I_1 and I_3 .
3. As the graph shows that $f^3(I_j) \supset I_j$, $j = 1, 2, 3$ and $f(I_1) \cap I_1 = \emptyset$ there is a three periodic orbit that moves among the three intervals.

Furthermore, it is easy to see that M^2 has no zero entries and therefore we know that the system has a *transitive orbit*.

The set of intervals we have chosen, it is good in the sense that it shows that there exist orbits of any period and also transitive orbits, but on the other hand, this choice does not show some important information. For instance, since the map crosses $y = x$ twice in I_3 , we know that there are two fixed points, but the transition graphs only point out one of them, in such interval. Consequently could be better to choose a finer partition of I , for instance usually it is a good idea to choose the relative extremis.

Proceeding in this way we get the new following intervals:

$$\begin{aligned} \tilde{I}_1 &= [0.946, 0.951], \quad \tilde{I}_2 = [0.951, 0.957], \quad \tilde{I}_3 = [0.957, 0.963], \\ \tilde{I}_4 &= [0.963, 0.97], \quad \tilde{I}_5 = [0.97, 0.975] \end{aligned}$$

See **Figure 14** and **Figure 15**

With this new graph we can see, for instance, that there are two fixed points in I_3 and that there is a total of three fixed points. The reason is that we have divided I_3 in \tilde{I}_4 and \tilde{I}_5 and it is verified that $f(\tilde{I}_i) \supset \tilde{I}_i$ for $i = 3, 4, 5$. Moreover, we have not lost the information about the 3-periodic orbit because $f^3(I_j) \supset I_j$, $j = 1, 4, 5$, and $f(\tilde{I}_1) = \tilde{I}_5$.

In addition, this new partition allows us to use symbolic dynamics to study it. In this case not all the words are admissible,

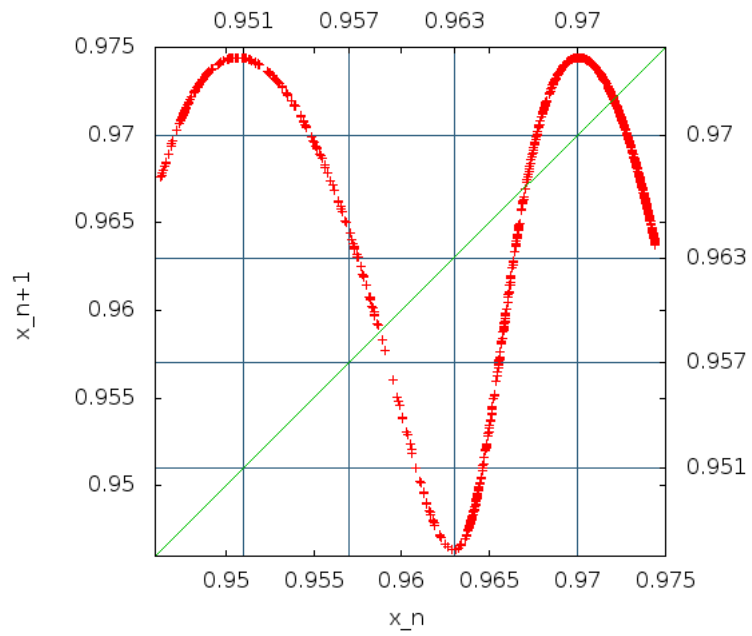


Figure 14: Transition graph for Poincaré map $x_{n+1} = P(x_n)$

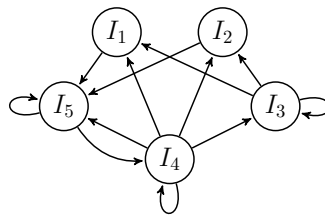


Figure 15: Transition graph for Poincaré map $x_{n+1} = P(x_n)$

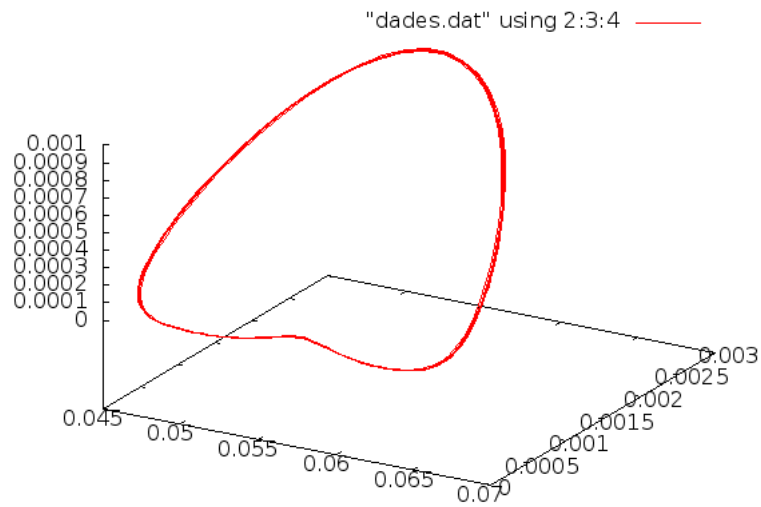


Figure 16: Stable focus

For the SEIR model a similar study can be done. The mechanism of transition to chaos is very similar: first a Hopf bifurcation, which creates a periodic orbit, then a cascade of period-doubling bifurcations of this periodic orbit, and later the appearance of a strange attractor if the system.

In **Figure 16** we show the stable focus, then in **Figure 17** we show the stable periodic orbit born in the Hopf bifurcation. **Figure 18** shows the strange attractor of the system.

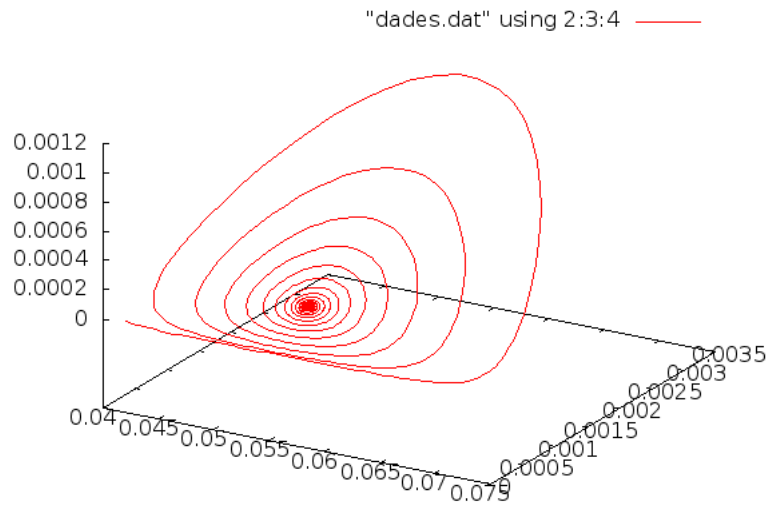


Figure 17: Stable periodic orbit

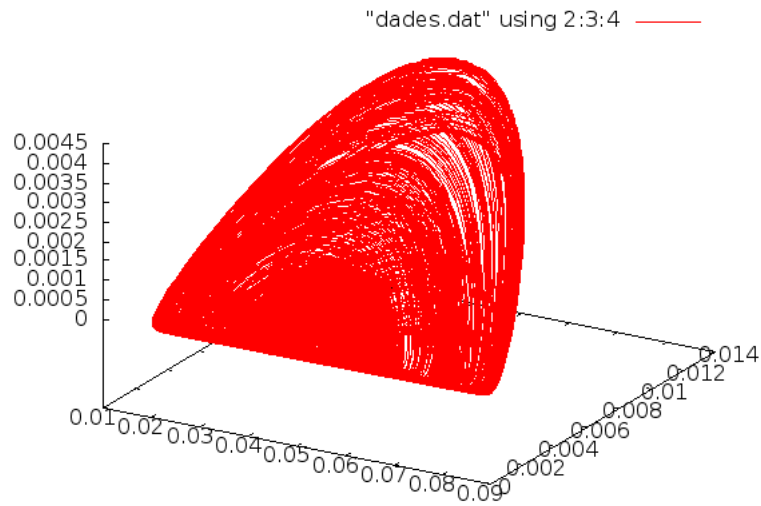


Figure 18: strange atractor

6 Chaos in real ecological systems

In this section we focus in the arguments the authors of the book [1] use to prove the existence of Chaos in real ecologic systems. As we already explained in the introduction, the use of mathematical models, as well as numerical simulation and other techniques coming from Dynamical Systems, have made apparent the fact that these systems can behave as deterministic chaotic systems.

Nevertheless, some groups of specialists in the area, still think that chaotic systems do not exist in nature by several reasons:

1. All the experiments done in labs with those species that are supposed to have chaotic behaviors seem to show the opposite behavior.
2. There is a mathematical-ecological argument: If the evolution of most of species is governed by deterministic chaos, as they pass through all the possible states of the systems, they should also become arbitrarily close to extinction. Therefore, if at those moment the cited species suffer some external pressure, they should disappear. This should be the cause of extinctions of a lot of species, but this is not the case.
3. There is a systematic doubt about the validity and the robustness of the mathematical models used. This has been often used as an evidence of that this chaotic behavior is a just "rare" property of the mathematical models themselves.

The two first objections can be overcome by using what is called the space-time chaos. In most of the models there is an implicit assumption: it is admissible to eliminate the space as a variable; the space makes to increase the number of individuals proportionally to the increasing of the space. But adding degrees of freedom to a complex and nonlinear system, as it is for instance the interaction of several populations, can lead to unsuspected behaviors.

The authors talk about experiments which results that show that, adding the space to a system leads to an increasing of its complexity. This can be, with high probability, one of the causes why species in nature, without space limitations, have a demographical evolution that seems governed by the deterministic chaos. But they do not show this chaotic behavior in more reduced spaces like a lab.

The same argument can be used for the second one. As we already notice, introducing time as a variable also increases the different qualitative dynamics in a system, and can make these dynamics more complex in general. But sometimes, the space variable can also have a stabilizing effect, is what the authors call the "chaotic stability". The meaning of this term can be understood as follows: If there is space between several groups of individuals of the same species, each can behave, up to certain point, as an independent system, having its own chaotic behavior and can reach some level close to extinction. Nevertheless at the same time other groups of the same species can be in a different state of the chaotic system, in such a way that sum of boths gives enough individuals to make the species survive.

The last objection is more difficult to refute. Nevertheless, there are other ways to prove or show signs of the existence of Chaos in natural systems and make this argument useless

En aquest sentit existeix un mètode molt interessant per a la reconstrucció de conjunts atractors d'un sistema, sobre el qual només es coneix la sèrie temporal d'alguna de les seves variables. S'anomena el mètode dels **delay plots**, utilitza el teorema de Whitney, desenvolupat per Takens:

Following wikipedia (http://en.wikipedia.org/wiki/Takens'_theorem):

A **delay embedding theorem** gives the conditions under which a chaotic dynamical system can be reconstructed from a sequence of observations of the state of a dynamical system. The reconstruction preserves the properties of the dynamical system that do not change under smooth coordinate changes, but it does not preserve the geometric shape of structures in phase space.

Takens theorem is the 1981 delay embedding theorem of Floris Takens. It provides the conditions under which a smooth attractor can be reconstructed from the observations made with a *generic function*. Later results replaced the smooth attractor with a set of arbitrary *box counting dimension* and the class of generic functions with other classes of functions.

Delay embedding theorems are simpler to state for discrete-time dynamical systems. The state space of the dynamical system is a ν -dimensional manifold M . The dynamics is given by a smooth map

$$f : M \rightarrow M$$

Assume that the dynamics f has a strange attractor A with box counting dimension d_A . Using ideas from *Whitney's embedding theorem*, A can be embedded in k -dimensional *Euclidean space* with

$$k > 2d_A$$

That is, there is a diffeomorphism φ that maps A into \mathbb{R}^k such that the derivative of φ has full rank.

A delay embedding theorem uses an "observation function" to construct the embedding function. An observation function α must be twice-differentiable and associate a real number to any point of the attractor A . It must also be typical, so its derivative is of full rank and has no special symmetries in its components. The delay embedding theorem states that the function

$$\phi_T(x) = (\alpha(x), \alpha(f(x)), \dots, \alpha(f^{k-1}(x)))$$

is an embedding of the strange attractor A .

There is a very interesting method to reconstruct attractors of a system, when we only know a temporal series of one of its variables. It is called the **Delay plots method**, and is a method based on Whitney theorem, that F. Takens developed in the 80s.

Following wikipedia (http://en.wikipedia.org/wiki/Takens'_theorem):

A **delay embedding theorem** gives the conditions under which a chaotic dynamical system can be reconstructed from a sequence of observations of the state of a dynamical

system. The reconstruction preserves the properties of the dynamical system that do not change under smooth coordinate changes, but it does not preserve the geometric shape of structures in phase space.

Takens theorem is the 1981 delay embedding theorem of Floris Takens. It provides the conditions under which a smooth attractor can be reconstructed from the observations made with a *generic function*. Later results replaced the smooth attractor with a set of arbitrary *box counting dimension* and the class of generic functions with other classes of functions.

Delay embedding theorems are simpler to state for discrete-time dynamical systems. The state space of the dynamical system is a ν -dimensional manifold M . The dynamics is given by a smooth map

$$f : M \rightarrow M$$

Assume that the dynamics f has a strange attractor A with box counting dimension d_A . Using ideas from *Whitney's embedding theorem*, A can be embedded in k -dimensional *Euclidean space* with

$$k > 2d_A$$

That is, there is a diffeomorphism φ that maps A into \mathbb{R}^k such that the derivative of φ has full rank.

A delay embedding theorem uses an "observation function" to construct the embedding function. An observation function α must be twice-differentiable and associate a real number to any point of the attractor A . It must also be typical, so its derivative is of full rank and has no special symmetries in its components. The delay embedding theorem states that the function

$$\phi_T(x) = (\alpha(x), \alpha(f(x)), \dots, \alpha(f^{k-1}(x)))$$

is an embedding of the strange attractor A .

Takens theorem shows that it is enough to have a temporal series of one of the variables of the system to reconstruct the rest of the needed information to rebuild the attractor. We just need to work with one variable and replace the other variables by the resulting time τ -delayed value of the chosen variable that we know by the temporal series.

For instance, if we have a n -dimensional dynamical system and we only know measures of a temporal series of a certain variable $x(t)$, we will build a phase space given by the variables:

$$\{x(t), x(t - \tau), x(t - 2\tau), \dots, x(t + (n - 1)\tau)\}$$

Using this method in cases where the temporal series comes from real data one has to rebuild an attractor that has the structure of a strange attractor. Of course, it is important to avoid the possible noise coming from wrong data, wrong measurements, or other factors that have no relation with the presence of a strange attractor in the real system. To this end, the used tool is the Poincaré map, also very used during this work. Moving the Poincaré section transversally to the orbits one can obtain the points given by the orbits when they meet the section. Looking at the "picture" this map defines a deterministic behavior, the same happens with the system. On the contrary, when the

system is chaotic, one can just see a kind of "cloud" of disordered points. Obviously, this last observation is not a rigorous proof of the existence or not of chaos, but it is a good way to obtain some evidence of it.

References

- [1] JORDI BASCOMPTE, JORDI FLOS(COORD.), EMILIA GUTIÉRREZ, DAVID JOU, RAMON MARGALEF, CARLES SIMÓ, RICARD V.SOLÉ, *Ordre i caos en ecologia*. Universitat de Barcelona 1995.
- [2] J. GUCKENHEIMER, P. HOLMES, *Nonlinear Oscillations, Dynamical Systems, and Bifurcations of Vector Fields*. Springer-Verlag. 1983.
- [3] A. HASTINGS, T. POWELL, *Chaos in Three-Species Food Chain Ecology*. 1991.
- [4] ROBERT L. DEVANEY, *Introduction to Chaotic Dynamical Systems* Addison-Wesley Publishing Company, Inc. 1989.
- [5] C. SIMÓ, *Global dynamics and fast indicators*. In H.W. Broer, B. Krauskopf, and G. Vegter, editors, *Global analysis of dynamical systems*, pages 373-389, Bristol, 2001. IOP Publishing
- [6] A. Jorba, M. Zou, *A software package for the numerical integration of ODE by means of high-order Taylor methods* 2001.
- [7] ALLIGOOD K.T., YORKE J.A, T.D.SAUER. , *Chaos.. An Introduction to Dynamical Systems*. 2009. Springer.
- [8] L.F. OLSEN, M. SCHAFFER , *Chaos versus noisy periodicity: alternative hypotheses for childhood epidemics*. Science 249, 1990: 499-504.
- [9] J. SOTOMAYOR *Lições de equações diferenciais ordinarias* IMPA 1979.